

# Erianin Controls Collagen-Mediated Retinal Angiogenesis via the RhoA/ROCK1 Signaling Pathway Induced by the $\alpha$ 2/ $\beta$ 1 Integrin-Collagen Interaction

Xueke Li, Xiaoxue Liu, Yue Xing, Lingyan Zeng, Xin Liu, Huangxuan Shen, and Jin Ma

State Key Laboratory of Ophthalmology, Zhongshan Ophthalmic Center, Sun Yat-sen University, Guangzhou, China

Correspondence: Jin Ma, Zhongshan Ophthalmic Center, Sun Yat-sen University, Guangzhou 510060, P.R. China; [zoc\\_majin@aliyun.com](mailto:zoc_majin@aliyun.com).

Xueke Li and Xiaoxue Liu contributed equally as co-first authors.

**Received:** June 30, 2021

**Accepted:** December 27, 2021

**Published:** January 21, 2022

Citation: Li X, Liu X, Xing Y, et al. Erianin controls collagen-mediated retinal angiogenesis via the RhoA/ROCK1 signaling pathway induced by the  $\alpha$ 2/ $\beta$ 1 integrin-collagen interaction. *Invest Ophthalmol Vis Sci.* 2022;63(1):27. <https://doi.org/10.1167/iovs.63.1.27>

**PURPOSE.** Erianin has been reported to inhibit tumor activity by suppressing the expression of integrins. It is hypothesized that erianin can inhibit retinal neovascularization in collagen by suppressing the expression of integrins. With an aim to test this hypothesis, the regulation of erianin on collagen-mediated retinal angiogenesis via the Ras homolog gene family member A (RhoA)/Rho-associated coiled-coil containing protein kinase 1 (ROCK1) signaling pathway induced by  $\alpha$ 2 and  $\beta$ 1 integrin-collagen interactions was investigated.

**METHODS.** The effects of erianin on human retinal vascular endothelial cells (HRVECs) were assessed in vitro using a hypoxia model in a three-dimensional cell culture induced by cobalt (II) chloride (CoCl<sub>2</sub>). A hypoxia-induced retinopathy model in adult zebrafish and zebrafish embryos was established to assess the antiangiogenic effect of erianin with and without vitreous collagen in vivo. The expression of  $\alpha$ 2 and  $\beta$ 1 integrin and RhoA/ROCK1 pathway in HRVECs and zebrafish retinas were analyzed.

**RESULTS.** In vitro, collagen improved the angiogenic potential of HRVECs, including migration, adhesion, and tube formation, in a three-dimensional cell culture model. Erianin suppressed the angiogenic processes of the CoCl<sub>2</sub>-induced hypoxia HRVEC model in a concentration-dependent manner. In vivo, erianin reduced retinal angiogenesis in the hypoxia-induced retinopathy model in adult and embryo zebrafish. Erianin inhibited the expression of  $\alpha$ 2 and  $\beta$ 1 integrin and RhoA/ROCK1 in a hypoxia-induced model in vitro in three-dimensional cell culture and in vivo in adult zebrafish.

**CONCLUSIONS.** Collagen-mediated retinal angiogenesis may be regulated by erianin via the RhoA/ROCK1 signaling pathway induced by  $\alpha$ 2 and  $\beta$ 1 integrin-collagen interactions. These findings suggest that erianin has the therapeutic potential on intraocular collagen-mediated retinal angiogenesis.

**Keywords:** erianin, retinal neovascularization, collagen,  $\alpha$ 2 and  $\beta$ 1 integrin, RhoA/ROCK1 pathway

Extracellular matrix (ECM) molecules play an important role in angiogenesis.<sup>1</sup> Many ECM molecules, including collagen, laminin, and fibronectin, have proangiogenic properties.<sup>2-6</sup> Vitreous is a hydrated ECM comprised primarily of collagens,<sup>7</sup> including collagens II, IX, and V/XI and type II collagen forms the main scaffold of the vitreous body and contribute to preretinal neovascularization.<sup>8</sup> Vitreous collagen provides a scaffold that is required for vascular endothelial cells to form not only blood vessels but also adhesion to specific ECM components via cell receptors, providing critical intracellular signaling required for angiogenic processes.<sup>9</sup> In our previous study, key angiogenesis processes, such as proliferation, migration, and adhesion of retinal vascular epithelial cells, were detected in a three-dimensional cell culture model in vitro, and  $\alpha$ 2 and  $\beta$ 1 integrin and RhoA/ROCK1 pathways appeared to be key mediators in the signaling pathways that control the proangiogenic effect of collagen in retinal angiogenesis.<sup>10</sup> The  $\alpha$ 2 $\beta$ 1 integrin is the cell surface receptor for collagens, which can

recognize collagens and activates the Ras homolog gene family member A / Rho-associated coiled-coil containing protein kinase 1 (RhoA/ROCK) signaling pathway, mediating cell proliferation, adhesion, migration, and a lot of cellular processes.<sup>11</sup> However, the regulatory factors and their molecular mechanisms remain unclear.

The present study investigated the mechanism of the proangiogenic effects of collagen in vivo and in vitro and explored the effects of the inhibitory factor erianin on collagen-induced neovascularization. Erianin is the major bibenzyl compound found in the traditional Chinese medicine *Dendrobium chrysotoxum* Lindl.<sup>12</sup> Experimental data demonstrate that erianin has therapeutic potential to inhibit tumor angiogenesis<sup>13,14</sup> and attenuate the development of diabetic retinopathy by inhibiting retinal angiogenesis.<sup>15</sup>

It was hypothesized that erianin could play an important role in retinal neovascular disease by inhibiting collagen-mediated integrin and RhoA/ROCK1 pathways. Therefore,

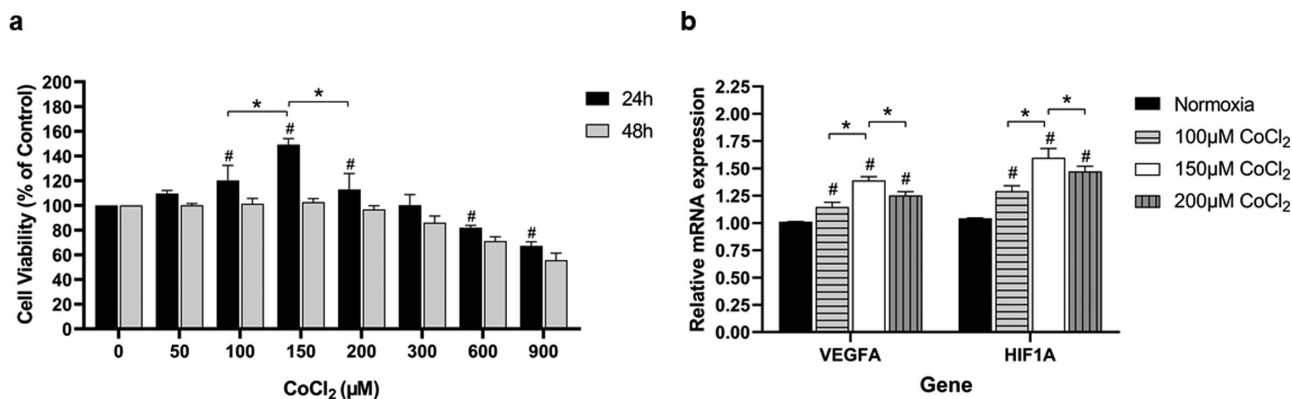


**FIGURE 1. Determination of CoCl<sub>2</sub> concentration for the cell hypoxia model.** (A) Cell proliferation was tested by CCK-8 assay. The 0nM CoCl<sub>2</sub> treated group was chosen as control. (B) The mRNA expression of VEGFA and HIF1A in HRVECs was tested after 24 hours of CoCl<sub>2</sub> exposure. Values are expressed as the mean  $\pm$  SD. VEGFA, vascular endothelial growth factor A; HIF1A, hypoxia-inducible factor 1-alpha. Normoxia group was set as the control at 100%. \* Significant difference among CoCl<sub>2</sub> with various concentrations (100  $\mu$ M, 150  $\mu$ M, and 200  $\mu$ M; paired *t*-test, *P* < 0.05). # Significant difference of CoCl<sub>2</sub> groups (100  $\mu$ M, 150  $\mu$ M, and 200  $\mu$ M) compared with the control normoxia group (paired *t*-test, *P* values < 0.05).

the inhibitory effect of erianin on collagen pro-angiogenesis in vivo and in vitro and its potential mechanisms were investigated in this study. In in vitro and in vivo studies, the hypoxic microenvironment plays a crucial role in angiogenesis. Although a decrease in oxygen concentration is the optimal hypoxia model, the problem faced by many researchers is access to a hypoxia chamber or a CO<sub>2</sub> incubator with regulated oxygen levels, which is not possible in many laboratories. Several alternative models have been used to mimic hypoxia. One of the most commonly used models is cobalt (II) chloride (CoCl<sub>2</sub>)-induced chemical hypoxia. There are numerous reports that CoCl<sub>2</sub> is the most widely used in various cultured cell lines and zebrafish hypoxia models.<sup>16–22</sup> CoCl<sub>2</sub> could induce the same hypoxia cell and zebrafish model just as those under low-oxygen condition,<sup>23–25</sup> which were utilized in this study.

## MATERIALS AND METHODS

### In Vitro Study

**Human Retinal Vascular Endothelial Cells Culture on Collagen.** Three-dimensional collagen gels were prepared according to Maritan et al.<sup>26</sup> by mixing ice-cold gel solutions at a final concentration of 1 mg/mL type I collagen (Corning, Tewksbury, MA, USA) to form gels. HRVECs (ACBRI-181; CSC, Kirkland, WA, USA) were cultured in 10% fetal bovine serum in Dulbecco's modified Eagle medium. HRVECs (10<sup>5</sup> cells/mL) were seeded on gels or plates. All cells were incubated in a humidified incubator at 37°C with 5% CO<sub>2</sub>.

**Angiogenic Processes Evaluation - Proliferation, Migration, Tube Formation, and Adhesion Assays.**

During the cell proliferation assays, HRVECs was incubated with Cell Counting Kit-8 (CCK-8) (Dojindo, Kumamoto, Japan) reagent solution and the absorbance at 450 nm was measured using a microplate reader (Bio-Tek Elx800, Bio-Tek, Winooski, VT, USA). During the migration assays, cells in the noncollagen culture were measured using a wound-healing assay and cells in collagen cultures were measured using the Transwell assay with the plate coated with type I collagen. Images were captured under

an inverted microscope (Nikon, Tokyo, Japan). The migrated area in wound healing assay and migrated cells in Transwell assay were quantified using ImageJ 1.52a software (National Institutes of Health [NIH], Bethesda, MD, USA). During the tube formation assay and adhesion assays, the upper surfaces of the 96-well plates were coated with Matrigel (Corning, Bedford, MA, USA) in the noncollagen group and coated with type I collagen in the collagen group. HRVECs were seeded in 96-well plates. In the tube formation assay, the plates were incubated for 12 hours to form capillary-like structures. The degree of tube formation was quantified by measuring the average branches of tubes using ImageJ software with the Angiogenesis Analyzer plugin 16. In the adhesion assay, HRVECs were incubated in the CO<sub>2</sub> incubator for 45 minutes. Nonadherent cells were removed, and adherent cells were fixed and the absorbance at 570 nm was measured using a microplate reader.

**Concentration Determination of CoCl<sub>2</sub> in the Cell Hypoxia Model.** Because cobalt is capable of mimicking hypoxia by causing inactivation of hydroxylase enzymes and stabilization of hypoxia-inducible factor-1, we applied CoCl<sub>2</sub> to induce hypoxia in cultured HRVECs. To determine the reasonable concentration and exposure time of CoCl<sub>2</sub> for inducing hypoxia in HRVECs, the cells were treated with various concentrations of CoCl<sub>2</sub> (0, 50, 100, 150, 200, 300, 600, and 900  $\mu$ M) for 24 hours and 48 hours. The cell proliferation improved significantly in the 100  $\mu$ M, 150  $\mu$ M, and 200  $\mu$ M concentration groups of CoCl<sub>2</sub> after 24 hours of exposure with the most obvious increase in 150  $\mu$ M CoCl<sub>2</sub> (Fig. 1A). Vascular endothelial growth factor A (VEGFA) and HIF1A were the major factors for cell proliferation stimulation. The mRNA expression of VEGFA and HIF1A in HRVECs was increased significantly in the 100  $\mu$ M, 150  $\mu$ M, and 200  $\mu$ M CoCl<sub>2</sub> groups after 24 hours of exposure with the most obvious increase in 150  $\mu$ M CoCl<sub>2</sub> (see Fig. 1B). Thus, CoCl<sub>2</sub> precultured or exposed to HRVECs at a concentration of 150  $\mu$ M for 24 hours was applied to establish a cell hypoxia model in the following study.

**Effects of Erianin on Angiogenic Processes In Vitro.** In all of the above assays, HRVECs were pretreated with 150  $\mu$ M CoCl<sub>2</sub> (Sigma, St. Louis, MO, USA) for 24 hours to mimic a hypoxic microenvironment. Erianin (Shanghai

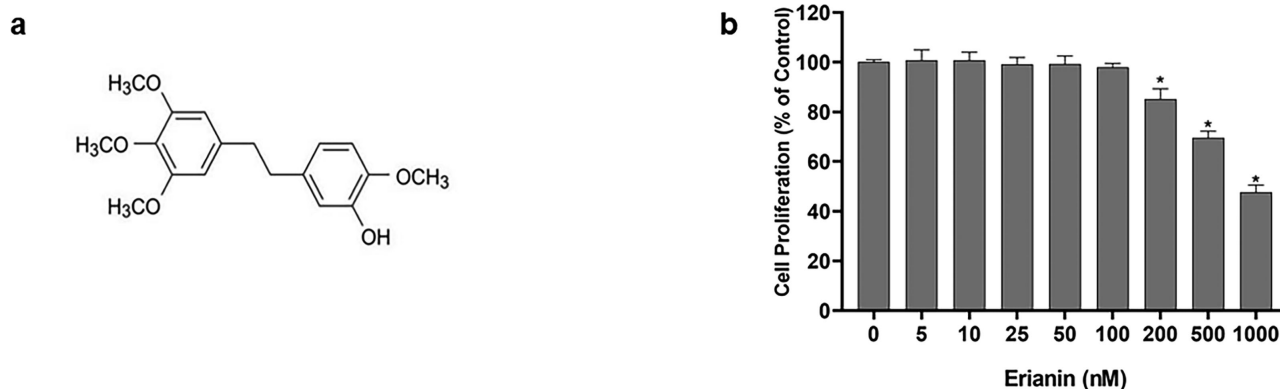


**FIGURE 2. The effect of erianin on the proliferation of HRVECs.** (A) Chemical structure of erianin. (B) The effect of erianin on the proliferation of HRVECs. Data are presented as percentages relative to the untreated control (0 nM erianin; % of control). \* Significant difference in erianin at various concentrations (200 nM, 500 nM, and 1000 nM) compared with the control group (paired *t*-test, *P* values < 0.05).

yuanye Bio-Technology Co., Shanghai, China; purity, 98.0%), molecular formula as Figure 2A, was made up in DMSO (Solarbio, Beijing, China) as a 25 mM stock solution. HRVECs were treated with different concentrations of erianin ranging from 5 to 1000 nM for cytotoxicity assay (see Fig. 2B) and screened for safe concentrations from 10 to 100 nM. Erianin at concentrations of 10 to 100 nM was added and HRVECs were analyzed by the same methods to observe the inhibitory effect on angiogenic processes.

### In Vivo Study

**Zebrafish Strains and Maintenance.** The *Tg (flk-GFP)* zebrafish used in this study were obtained from the Zebrafish Model Animal Facility at the Institute of Clinical and Translational Research of Sun Yat-sen University. Approximately 5 to 18 months old adult zebrafish were used for experiments in the collagen group and maintained in tap water at 28.5°C. Zebrafish embryos were collected at 1-day post-fertilization (dpf) for experiments in the noncollagen group. Before experimental operations, all zebrafish were anaesthetized with 0.02% tricaine (Sigma, St. Louis, MO, USA). This study was conducted in strict accordance with the recommendations stated in the Guide for the Care and Use of Laboratory Animals of the National Institutes of Health. The experiment protocol was approved by the Ethics Committee of Zhongshan Ophthalmic Center, Sun Yatsen University.

### Hypoxia-Induced Retinopathy Models in Zebrafish.

**CoCl<sub>2</sub>-Induced Hypoxia Retinopathy Model in Zebrafish Embryos.** To establish chemically induced hypoxia and neovascularization, 5 mM CoCl<sub>2</sub> was used at 1 dpf to stimulate abnormal embryonic retinal angiogenesis. The 5-dpf embryos were anesthetized in 0.02% tricaine in fish water and zebrafish embryonic eyes were isolated by intense shaking. Eyes were mounted in a glass-bottomed imaging dish and retinal vascular branching points and buds were observed under a 40 × objective of a Zeiss LSM 710 confocal microscope (Carl Zeiss Inc., Oberkochen, Germany).

**Low Oxygen-Induced Retinopathy Model in Adult Zebrafish.** The protocol for low oxygen exposure of adult zebrafish have been described previously.<sup>27</sup> Briefly, adult zebrafish were kept in water with a relative air saturation

of 10% for 7 days. After the zebrafish were euthanized, the fish eyes were dissected to isolate the retina. The retina was carefully divided evenly into four quadrants with no lost tissue fragments. Retinal neovascularization was visualized by a Zeiss LSM 710 confocal microscope and quantified by Angio Tool 64 0.6a software (SAIC-Frederick Inc., Frederick, MD, USA), as described previously.<sup>22,27</sup> The increase in retinal neovascularization under low oxygen demonstrates that the model was established successfully.

**Effects of Erianin on Angiogenesis In Vivo.** The effect of various concentrations of erianin (100, 200, 500, and 1000 nM) on retinal angiogenesis in vivo were evaluated in hypoxia-induced retinopathy models in zebrafish. In the embryo model, zebrafish embryos were exposed to embryo medium contains various concentrations (0–1000 nM) of erianin and 5 mM CoCl<sub>2</sub> at 1 dpf. After 4 days of exposure to erianin, developmental changes in embryonic retinal vessels were observed in one randomly selected eye. In the adult model, various concentrations (0–1000 nM) of erianin were injected into the vitreous cavity of the left eye, and the right eye was served as the paired control group. Retinal specimens were observed 7 days after erianin exposure. Retinal vessel branch points, numbers of sprouts, vessel diameters, and total vascularization areas were assessed using ImageJ software.

### Expression of $\alpha 2$ and $\beta 1$ Integrin and the RhoA/ROCK1 Pathway In Vitro and In Vivo

To investigate the mechanism of erianin on retinal neovascularization, we evaluated the gene and protein levels of  $\alpha 2$  and  $\beta 1$  integrins and the activation status of the RhoA/ROCK1 pathway.

**Real-Time PCR.** RNA isolation and semiquantitative RT-PCR were performed as described previously.<sup>28</sup> The relative expression of target genes was normalized to  $\beta$ -actin, analyzed by the 2<sup>- $\Delta\Delta$ Ct</sup> method and given as a ratio compared with the control. The primer sequences used in this study are shown in Tables 1 and 2.

**Rho GTPase Pull-Down Assay.** Rho activation in cultured cells was assessed as previously described.<sup>29,30</sup> The cells were lysed on ice in lysis buffer. The lysates were incubated with the glutathione S-transferase-rhotekin-Rho-

TABLE 1. Primer Sequences of In Vitro Study

Gene	Species	Primer	
<i>itga2</i>	Human	Forward	5'-AGACGTGCTCTTGGTAGGTG-3'
		Reverse	5'-GCTGACCCAAAATGCCCTCT-3'
<i>itgb1</i>	Human	Forward	5'-CGCGCGGAAAAGATGAATT-3'
		Reverse	5'-CACAAATTTGGCCCTGCTTGT-3'
<i>rhoa</i>	Human	Forward	5'-CCAGAGGTGTATGTGCCAC-3'
		Reverse	5'-ACAAAGCCAACCTACTCTGCT-3'
<i>rock1</i>	Human	Forward	5'-GGTGGTCCGTTGGGGTATTTT-3'
		Reverse	5'-CTCACTCCCTGTCAGTAAGGA-3'
<i>mypt1</i>	Human	Forward	5'-CCAGAGGTGTATGTGCCAC-3'
		Reverse	5'-ACAAAGCCAACCTACTCTGCT-3'
<i>actb1</i>	Human	Forward	5'-CTCCATCCTGGCCTCGCTGT-3'
		Reverse	5'-GCTGTACCTTACCCTCC-3'

*itga2*, integrin subunit alpha 2; *itgb1*, integrin subunit beta 1; *rhoa*, ras homologue gene family, member A; *rock1*, Rho-associated, coiled-coil containing protein kinase 1; *mypt1*, Myosin phosphatase target subunit 1; *actb1*, actin, beta 1.

TABLE 2. Primer Sequences of In Vivo Study

Gene	Species	Primer	
<i>itgb1</i>	Zebrafish	Forward	5'-CGTTTACCTCCGACTCCAACAATG-3'
		Reverse	5'-CTGTTCCACTCACTCCGTTCTTGC-3'
<i>itga2</i>	Zebrafish	Forward	5'-CGCTGCTGATTATCGAGGCTGAG-3'
		Reverse	5'-CTGACCACACCAAGGCACTG-3'
<i>rhoa</i>	Zebrafish	Forward	5'-AAGAGGACTACGACAGGCTGAGG-3'
		Reverse	5'-GGCGTCCATTCTCTGGGATGTTTC-3'
<i>rock1</i>	Zebrafish	Forward	5'-GCATTCGAAGACGACCGCTACC-3'
		Reverse	5'-GCACAACCTCCGAGTGTAGAAG-3'
<i>mypt1</i>	Zebrafish	Forward	5'-AAGAGGACTACGACAGGCTGAGG-3'
		Reverse	5'-GGCGTCCATTCTCTGGGATGTTTC-3'
<i>actb1</i>	Zebrafish	Forward	5'-CGCTGGTGCTGTTATGCTCTC-3'
		Reverse	5'-GCCATCAGGTCACATACACGGTTG-3'

*itga2*, integrin subunit alpha 2; *itgb1*, integrin subunit beta 1; *rhoa*, ras homologue gene family, member A; *rock1*, Rho-associated, coiled-coil containing protein kinase 1; *mypt1*, Myosin phosphatase target subunit 1; *actb1*, actin, beta 1.

binding domain previously bound to glutathione-Sepharose beads. Associated GTP-bound forms of Rho were released with SDS-polyacrylamide (SDS-PAGE) gel electrophoresis loading buffer and analyzed by Western blot analysis using a monoclonal antibody against RhoA.

**Western Blot Analysis.** The protein extracts of the HRVECs and zebrafish retinas were run on SDS-PAGE gels and transferred to polyvinylidene difluoride (PVDF) membranes, which were then incubated with primary antibodies against  $\alpha 2$  integrin (ab133557),  $\beta 1$  integrin (ab179471), RhoA (ab86297), ROCK1 (ab134181; Abcam, Cambridge, UK), MYPT1 (D6C1), phosphomyosin phosphatase targeting subunit 1 (p-MYPT1; Thr696), or  $\beta$ -actin (D6A8; Signaling Technology, Danvers, MA, USA), followed by secondary antibody incubation. The membranes were incubated with the corresponding secondary antibodies (Bioworld Technology Company, Nanjing, Jiangsu, China) the next day.

**Statistical Analysis.** The data were obtained from at least three independent experiments and are presented as the mean  $\pm$  standard deviation (SD). In an in vitro study, cells cultured under the same collagen or noncollagen conditions were compared by paired *t*-test, and the cells were cultured under different condition (between collagen and noncollagen) were compared by independent sample *t*-tests. In the in vivo study, the paired *t*-test was taken in the study of adult

zebrafish, and the independent sample *t*-tests were taken in zebrafish embryos. Inhibition rate of cell proliferation and tube formation were calculated for comparison by paired *t*-test between hypoxic HRVECs cultured under collagen and noncollagen conditions.

The test level was  $\alpha = 0.05$ , with  $P < 0.05$  considered significant. SPSS version 25.0 (SPS Inc., Chicago, IL, USA) was used for all statistical analyses.

## RESULTS

### In Vitro: Antiangiogenic Effect of Erianin on HRVECs

**Concentration Determination of CoCl<sub>2</sub> in the Cell Hypoxia Model.** Because cobalt is capable of mimicking hypoxia by causing inactivation of hydroxylase enzymes and stabilization of hypoxia-inducible factor-1, we applied CoCl<sub>2</sub> to induce hypoxia in cultured HRVECs. To determine the reasonable concentration and exposure time of CoCl<sub>2</sub> for inducing hypoxia in HRVECs, the cells were treated with various concentrations of CoCl<sub>2</sub> (0, 50, 100, 150, 200, 300, 600, and 900  $\mu$ M) for 24 hours and 48 hours. The cell proliferation improved significantly in the 100  $\mu$ M, 150  $\mu$ M, and 200  $\mu$ M concentration groups of CoCl<sub>2</sub> after 24 hours of exposure with the most obvious increase in 150  $\mu$ M CoCl<sub>2</sub> (see Fig. 1A). The VEGFA and HIF1A were the major factors for cell proliferation stimulation.<sup>31</sup> The mRNA expression of VEGFA and HIF1A in HRVECs was increased significantly in the 100  $\mu$ M, 150  $\mu$ M, and 200  $\mu$ M CoCl<sub>2</sub> groups after 24 hours of exposure with the most obvious increase in 150  $\mu$ M CoCl<sub>2</sub> (see Fig. 1B). Thus, CoCl<sub>2</sub> precultured or exposed to HRVECs at a concentration of 150  $\mu$ M for 24 hours was applied to establish a cell hypoxia model in the following study.

**Effect of Erianin on Angiogenic Processes of Hypoxic HRVECs Cytotoxicity Evaluation of Erianin on HRVECs.** First, to determine the appropriate treatment dose of erianin with no cytotoxicity, various concentrations of erianin (0, 5, 10, 25, 50, 100, 200, 500, and 1000 nM) were applied to HRVECs for 24 hours. Erianin did not cause cytotoxic effects on HRVECs at concentrations up to 100 nM (see Fig. 2B). Therefore, in vitro angiogenesis assays using HRVECs were performed at treatment concentrations of less than 100 nM erianin.

**Inhibition of Hypoxic HRVEC Proliferation by Erianin.** The proliferation of collagen-cultured hypoxic HRVECs was inhibited significantly more by erianin at various concentrations (25, 50, and 100 nM) compared with the CoCl<sub>2</sub> group without erianin treatment. Erianin exerted a dose-dependent inhibition of cell proliferation from 10 nM to 100 nM (Fig. 3A). The inhibition rate of hypoxic cell proliferation was increased more significantly by erianin at various concentrations (50 and 100 nM) in the collagen-cultured groups than in the noncollagen group (see Fig. 3B).

**Inhibition of Hypoxic HRVEC Migration by Erianin.** Transwell assays were used to assess the effect of erianin on HRVEC migration in collagen culture (Fig. 4A). Wound healing assays were used to assess the effect of erianin on HRVEC migration in noncollagen culture (see Fig. 4B). The migration of collagen- and noncollagen-cultured hypoxic HRVECs was inhibited more significantly by erianin at various concentrations (10, 25, 50, and 100 nM) than by 0 nM erianin. Erianin exerted a dose-dependent inhibition on cell migration in the collagen group and noncollagen groups

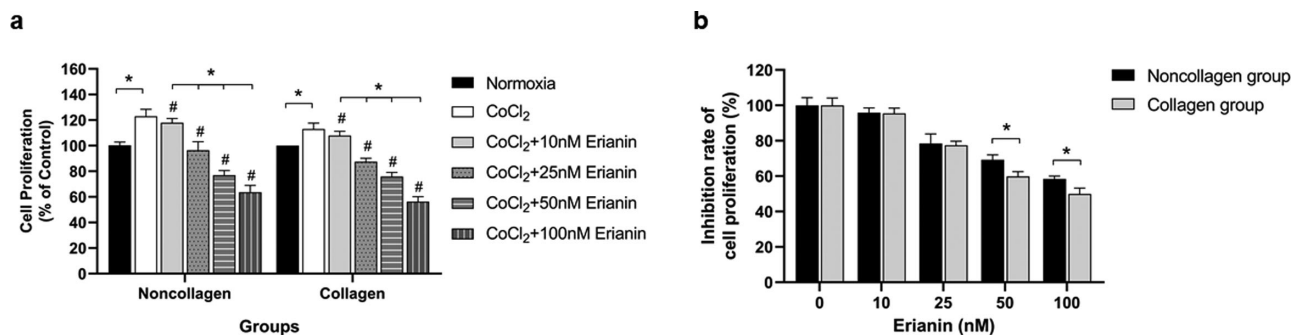


**FIGURE 3. Effect of erianin on the proliferation of HRVECs induced by CoCl<sub>2</sub> for 24 hours.** Cell proliferation was determined by CCK-8 assay. (A) HRVECs were treated with erianin at various concentrations (0–100 nM). Comparison of the inhibition rate of cell proliferation among collagen groups and among noncollagen groups. The normoxia group without erianin treatment was set as the control at 100%. (B) The inhibition rate of cell proliferation was compared between hypoxic HRVECs cultured under collagen and noncollagen conditions. Hypoxic cells without erianin treatment were set as the control at 100%. \* Significant difference between samples (paired *t*-test, *P* values < 0.05); # Significant difference compared with CoCl<sub>2</sub>-incubated cells without erianin treatment (paired *t*-test, *P* values < 0.05). † Significant difference between collagen- and noncollagen-culture groups (independent sample *t*-test, *P* values < 0.05).

in the 10 nM to 100 nM erianin concentration groups (see Fig. 4C).

**Inhibition of Hypoxic HRVEC Tube Formation by Erianin.** Following stimulation by CoCl<sub>2</sub>, collagen-cultured HRVECs became aligned into cords, and a tube-like structure was formed (Fig. 5A). HRVECs seeding on the Matrigel were used to assess the effect of erianin on tube formation of HRVECs in the noncollagen group (see Fig. 5B). Tube formation of collagen- and noncollagen-cultured hypoxic HRVECs was inhibited more significantly by erianin at various concentrations (10, 25, 50, and 100 nM) than by 0 nM erianin (see Fig. 5C). Erianin exerted a dose-dependent inhibition of cell tube formation from 10 nM to 100 nM (see Fig. 5A, 5C). After comparing the collagen and noncollagen groups, the inhibition rate of hypoxic cell tube formation was inhibited more significantly by erianin exposure at various concentrations (25, 50, and 100 nM) in the collagen group than in the noncollagen group (see Fig. 5D).

**Inhibition of Hypoxic HRVEC Adhesion by Erianin.** Adhesion of collagen-cultured hypoxic HRVECs was inhibited more significantly by erianin exposure at various concentrations (10, 25, 50, and 100 nM) than by 0 nM erianin exposure. Erianin exerted a dose-dependent inhibition of cell adhesion from 10 nM to 100 nM (Fig. 6).

### In Vivo: Effect of Erianin on Hypoxia-Induced Retinal Neovascularization in Zebrafish

**Low Oxygen-Induced Retinal Neovascularization in Adult Zebrafish.** The retinal capillary plexuses of retinal arterioles and veins formed new sprouts that grew to a high density of capillary networks over 14 days in the low oxygen group compared with the normoxia group (Figs. 7a–c). Quantification analysis of vascular branches, sprouts, and vascularization areas of the total retina and high vascularity areas of the retina after exposure to low oxygen showed significant increase compared with the normoxia group, suggesting that a retinal neovascularization model was established (see Figs. 7A, 7B).

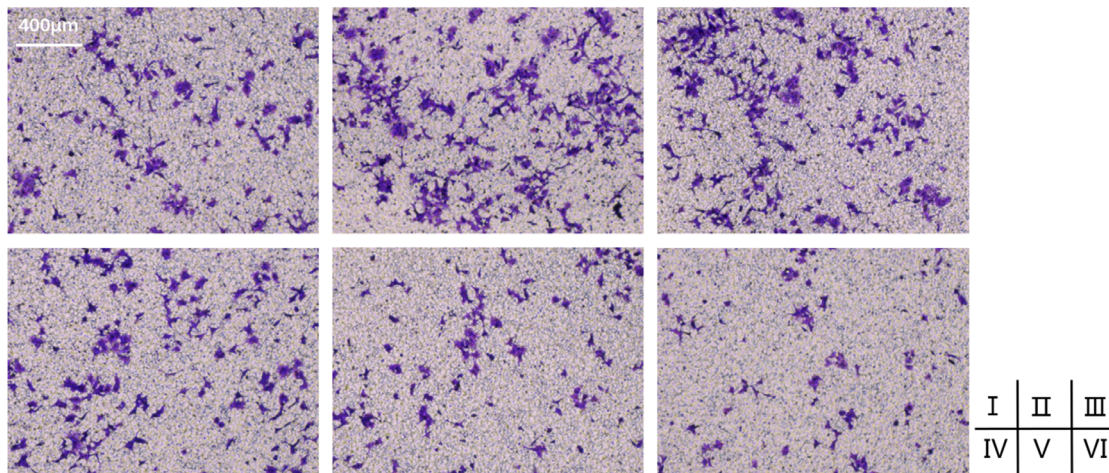
**Effect of Erianin on Low Oxygen-Induced Retinal Neovascularization in Adult Zebrafish.** All adult zebrafish retinas were exposed to various concentrations

of erianin (0, 100, 200, 500, and 1000 nM) for 7 days, and retinal branch points, sprouts, thickness, and vascularization areas were observed. After comparison with the 0 nM erianin concentration group, various concentrations of erianin (100, 200, 500, and 1000 nM) showed approximately 7%, 15%, 20%, and 28% reduction in low oxygen-induced vessel branch points of the total retina, 10%, 19%, 26%, and 32% reduction in vessel sprouts and 9%, 18%, 25%, and 30% in vascularization areas, and 18%, 35%, 54% and 64% reduction in low oxygen-induced vessel branch points of high vascularity areas of the retina, 10%, 19%, 26%, and 32% reduction in vessel sprouts and 8%, 17%, 36%, and 48% in vascularization areas, respectively. Meanwhile, after comparison with the 0 nM erianin concentration group, various concentrations of erianin (100, 200, 500, and 1000 nM) showed approximately 7%, 5%, 8%, and 9% reduction in low oxygen-induced vessel thickness of the total retina, and 6%, 8%, 11%, and 12% reduction in high vascularity areas of the retina, respectively. Erianin exerted a dose-dependent inhibition on low oxygen-induced retinal vessel branches, sprouts, and vascularization areas from 200 nM to 1000 nM in both the total retina and high vascularity areas of the retina (Figs. 8A, 8B). However, the difference in retinal vessel thickness between different concentrations of erianin was not statistically significant (independent sample *t*-test, *P* values > 0.05).

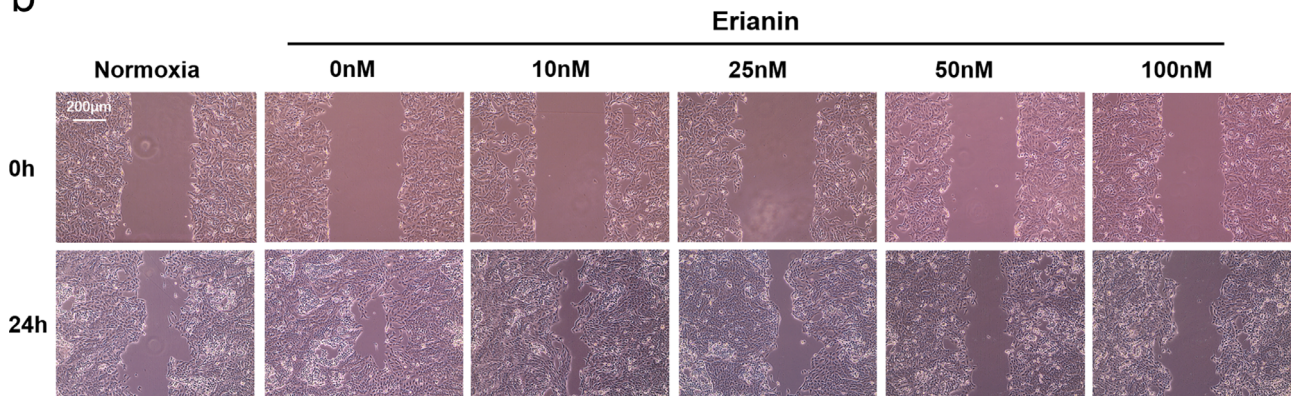
**CoCl<sub>2</sub>-Induced Retinal Neovascularization in Zebrafish Embryos.** We treated embryos with 5 mM CoCl<sub>2</sub> for 5 days to establish a model of CoCl<sub>2</sub>-induced retinal neovascularization according to previous research.<sup>22</sup> A confocal examination of 5 mM CoCl<sub>2</sub>-treated zebrafish embryos at 5 dpf revealed an increased number of vascular branch points and dilated vessels compared with that in the control group (Figs. 9A, 9B). Compared with the experimental controls (0 mM CoCl<sub>2</sub>), *vegfaa* and *vegfr2* expression significantly increased at 5 dpf in the CoCl<sub>2</sub>-treated embryos (see Fig. 9B). Overexpression of *vegfaa* and *vegfr2* mRNA was consistent with hypoxia, indicating that CoCl<sub>2</sub>-induced hypoxia is suitable for a retinal neovascularization model in zebrafish embryos.

**Effect of Erianin on CoCl<sub>2</sub>-Induced Retinal Neovascularization in Zebrafish Embryos.** All zebrafish embryos were exposed to various concentrations of erianin (0, 100, 200, 500, and 1000 nM) for 4 days, and

a



b



c

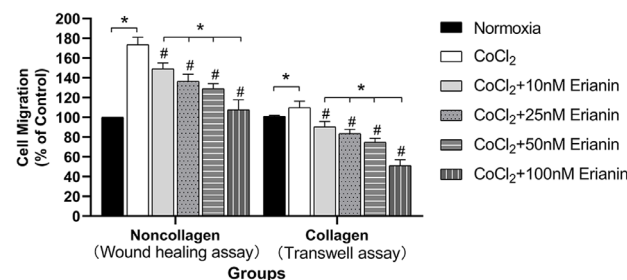


**FIGURE 4. Effect of erianin on HRVEC migration.** (A) Collagen-cultured hypoxic HRVEC migration was evaluated by Transwell assay (100 ×). (I) Cells without CoCl<sub>2</sub> and erianin exposure; (II) cells with CoCl<sub>2</sub> and without erianin exposure; hypoxic cells exposed to erianin at various concentrations of 10 nM (III), 25 nM (IV), 50 nM (V), and 100 nM (VI). (B) Cell migration of noncollagen-cultured HRVECs evaluated by wound healing assays (100 ×). (C) Comparison of the inhibition rate of cell migration among collagen groups and among noncollagen groups. The normoxia group was set as the control at 100%. \* Significant difference between samples (paired *t*-test, *P* values < 0.05); # Significant difference compared with CoCl<sub>2</sub>-incubated cells without erianin treatment (paired *t*-test, *P* values < 0.05).

the retinal vessel diameter, sprouts, branch points, and thickness were observed (Fig. 10A). Compared with the 0 nM erianin concentration group, various concentrations of

erianin (100, 200, 500, and 1000 nM) showed approximately 10%, 15%, 28%, and 40% reductions in CoCl<sub>2</sub>-induced retinal vessel branch points, 18%, 24%, 32%, and 47% reductions in

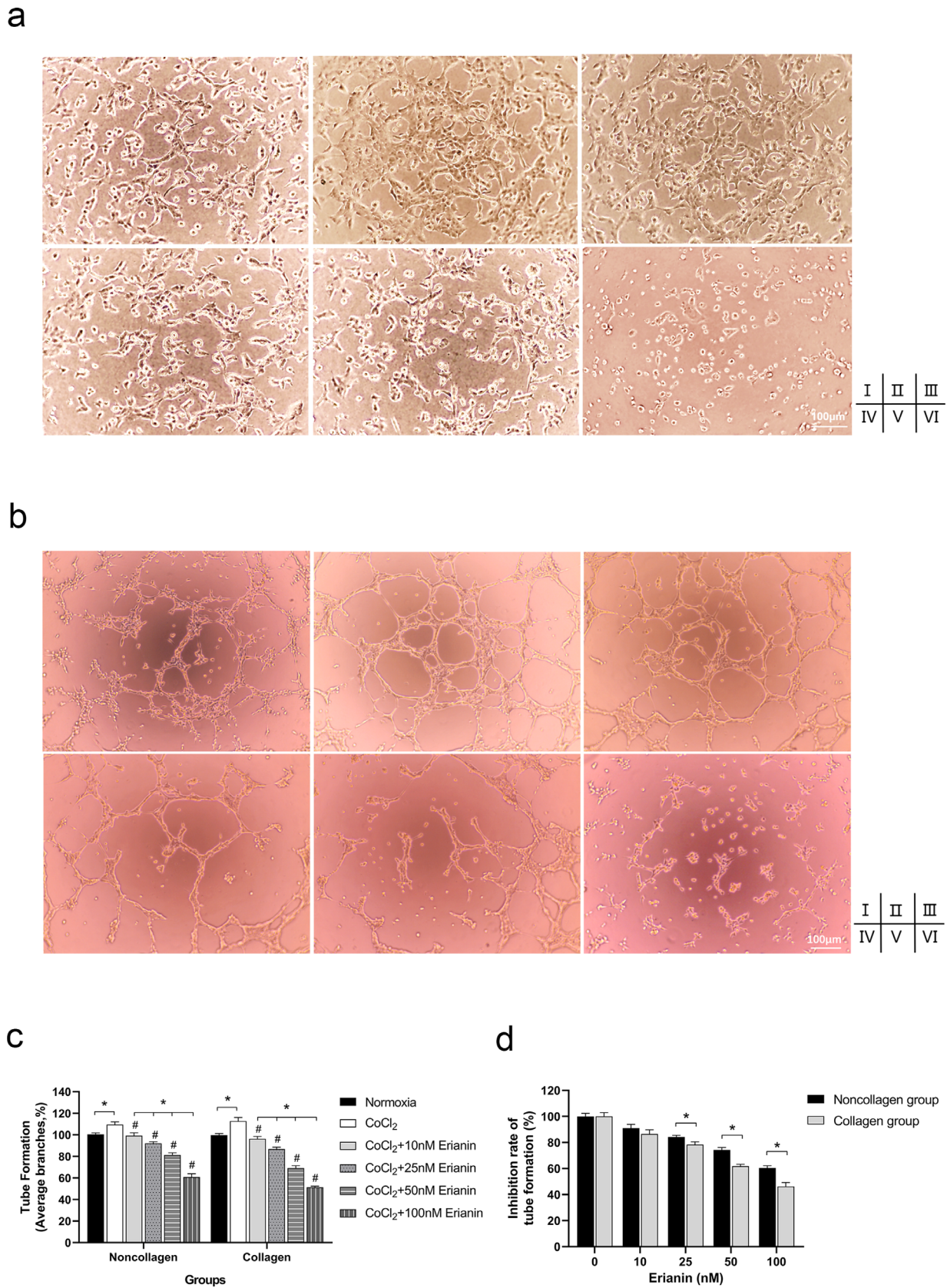


**FIGURE 5. Effect of erianin on tube formation of HRVECs. (A)** Tube formation of collagen-cultured HRVECs exposed to DMEM (I), CoCl<sub>2</sub> (II), or erianin at various concentrations (10 nM [III], 25 nM [IV], 50 nM [V], and 100 nM [VI]) [100 ×]. **(B)** Tube formation of noncollagen-cultured HRVECs exposed to DMEM (I), CoCl<sub>2</sub> (II), or erianin at various concentrations (10 nM [III], 25 nM [IV], 50 nM [V], 100 nM [VI]) 100 ×). **(C)** Comparison of cell tube formation among collagen groups and among noncollagen groups. The normoxia group was set as the control at 100%. **(D)** The inhibition rate of tube formation was compared between hypoxic HRVECs cultured under collagen and noncollagen

conditions. Hypoxic cells without erianin treatment were set as the controls at 100%. \* Significant difference between samples (paired *t*-test, *P* values < 0.05); # Significant difference compared with CoCl<sub>2</sub>-incubated cells without erianin treatment (paired *t*-test, *P* values < 0.05); † Significant difference between collagen- and noncollagen-culture group (independent sample *t*-test, *P* values < 0.05).

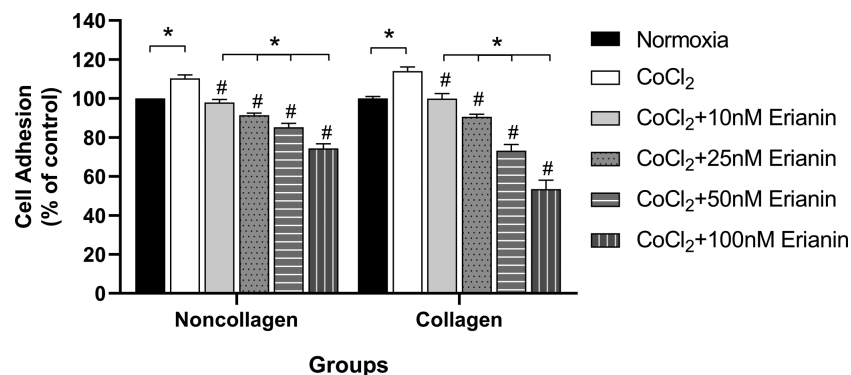


**FIGURE 6. Effect of erianin on HRVEC adhesion.** Comparison of cell adhesion ability in each collagen- and noncollagen-culture groups. The normoxia group was set as the control at 100%. \* Significant difference between samples (paired *t*-test, *P* values < 0.05); # Significant difference compared with CoCl<sub>2</sub>-incubated cells without erianin treatment (paired *t*-test, *P* values < 0.05).

vessel diameter, 14%, 28%, 35%, and 53% in vessel sprouts, and 10%, 12%, 14%, and 18% in vessel thickness, respectively. Erianin at a 1000 nM concentration exerted significant inhibition on CoCl<sub>2</sub>-induced retinal vessel branches, vessel sprouts, and dilated vessels compared with the 200 nM concentration groups, whereas there was no statistically significant difference in vessel thickness (independent sample *t*-test, *P* values > 0.05; see Fig. 10B).

### Effects of Erianin on $\alpha 2$ and $\beta 1$ Integrins and the RhoA/ROCK1 Pathway

**Effects of Erianin on  $\alpha 2$  and  $\beta 1$  Integrins In Vitro.** To determine the mechanism of erianin in collagen-cultured hypoxic HRVECs, in an in vitro study, we evaluated the levels of  $\alpha 2$  and  $\beta 1$  integrins, receptors on collagen-cultured HRVECs. The mRNA and protein expression of  $\alpha 2$  and  $\beta 1$  integrins in HRVECs were higher in the collagen group than in the noncollagen group. Both the mRNA and protein expression of  $\alpha 2$  and  $\beta 1$  integrins in CoCl<sub>2</sub>-stimulated HRVECs were the same as those in the normoxia group. Compared with 0 nM erianin, various concentrations of erianin (25, 50, and 100 nM) significantly decreased the mRNA and protein levels of  $\alpha 2$  and  $\beta 1$  integrins in hypoxic cells in both the collagen and noncollagen groups. Erianin dose-dependently inhibited the mRNA and protein levels of  $\alpha 2$  and  $\beta 1$  integrins from 10 nM to 100 nM (Figs. 11A, 11B). After comparing the collagen and noncollagen groups, we found that the inhibition ratios of mRNA and protein levels in hypoxic cells were decreased more significantly by various concentrations of erianin (25, 50, and 100 nM) in the collagen groups than in the noncollagen group (see Fig. 11C).

**Effects of Erianin on  $\alpha 2$  and  $\beta 1$  Integrins In Vivo.** In an in vivo study, we evaluated the mRNA and protein levels of  $\alpha 2$  and  $\beta 1$  integrins in the zebrafish retinas of adults and embryos. Under normoxic conditions, the mRNA and protein expression of  $\alpha 2$  and  $\beta 1$  integrins in the retina was higher in adult zebrafish than in zebrafish embryos. Under hypoxic conditions, the mRNA and protein levels of

$\alpha 2$  and  $\beta 1$  integrins in the retina were the same as those in normoxic retinas in both adult zebrafish and zebrafish embryo. Compared with 0 nM erianin, various concentrations of erianin (200, 500, and 1000 nM) significantly inhibited the mRNA and protein levels of  $\alpha 2$  and  $\beta 1$  integrins in the retinas of adult and embryonic zebrafish under hypoxic conditions. Erianin dose-dependently inhibited the mRNA and protein levels of  $\alpha 2$  and  $\beta 1$  integrins in the retinas of adult zebrafish and zebrafish embryos at concentrations from 100 nM to 1000 nM (Figs. 12A, 12B). After comparing the adult and embryos groups, we found that the inhibition of *itga2* and *itgb1* in the adult zebrafish retina by various concentrations of erianin (200, 500, and 1000 nM) and the inhibition of protein levels of  $\alpha 2$  and  $\beta 1$  integrins by various concentrations of erianin (500 and 1000 nM) were decreased more significantly under hypoxic conditions than in zebrafish embryos (see Fig. 12C).

**Effects of Erianin on the RhoA/ROCK1 Pathway In Vitro.** We also evaluated the activation status of the RhoA/ROCK1 pathway by assessing the active GTP-RhoA, ROCK1, and p-MYPT1. In the in vitro study, the activity of RhoA and ROCK1 in HRVECs under normoxic conditions were significantly increased in the collagen group compared with the noncollagen group. The mRNA and protein levels of RhoA, ROCK1, and MYPT1 in CoCl<sub>2</sub>-stimulated HRVECs were the same as those in normoxia-stimulated HRVECs in both the collagen and noncollagen groups (Figs. 13A, 13B). There were no significant differences in RhoA, ROCK1, and MYPT1 gene expression in hypoxic cells by various concentration of erianin (see Fig. 13A). In the collagen group, various concentrations of erianin (25, 50, and 100 nM) significantly decreased the activity of RhoA and ROCK1 in CoCl<sub>2</sub>-stimulated HRVECs compared with 0 nM erianin. Erianin dose-dependently inhibited the activity of RhoA and ROCK1 from 10 nM to 100 nM (see Fig. 13B). In the noncollagen group, erianin had no significant effect on the activity of RhoA and ROCK1 in CoCl<sub>2</sub>-stimulated HRVECs (see Fig. 13A).

**Effects of Erianin on the RhoA/ROCK1 Pathway In Vivo.** In an in vivo study, the activity of RhoA and

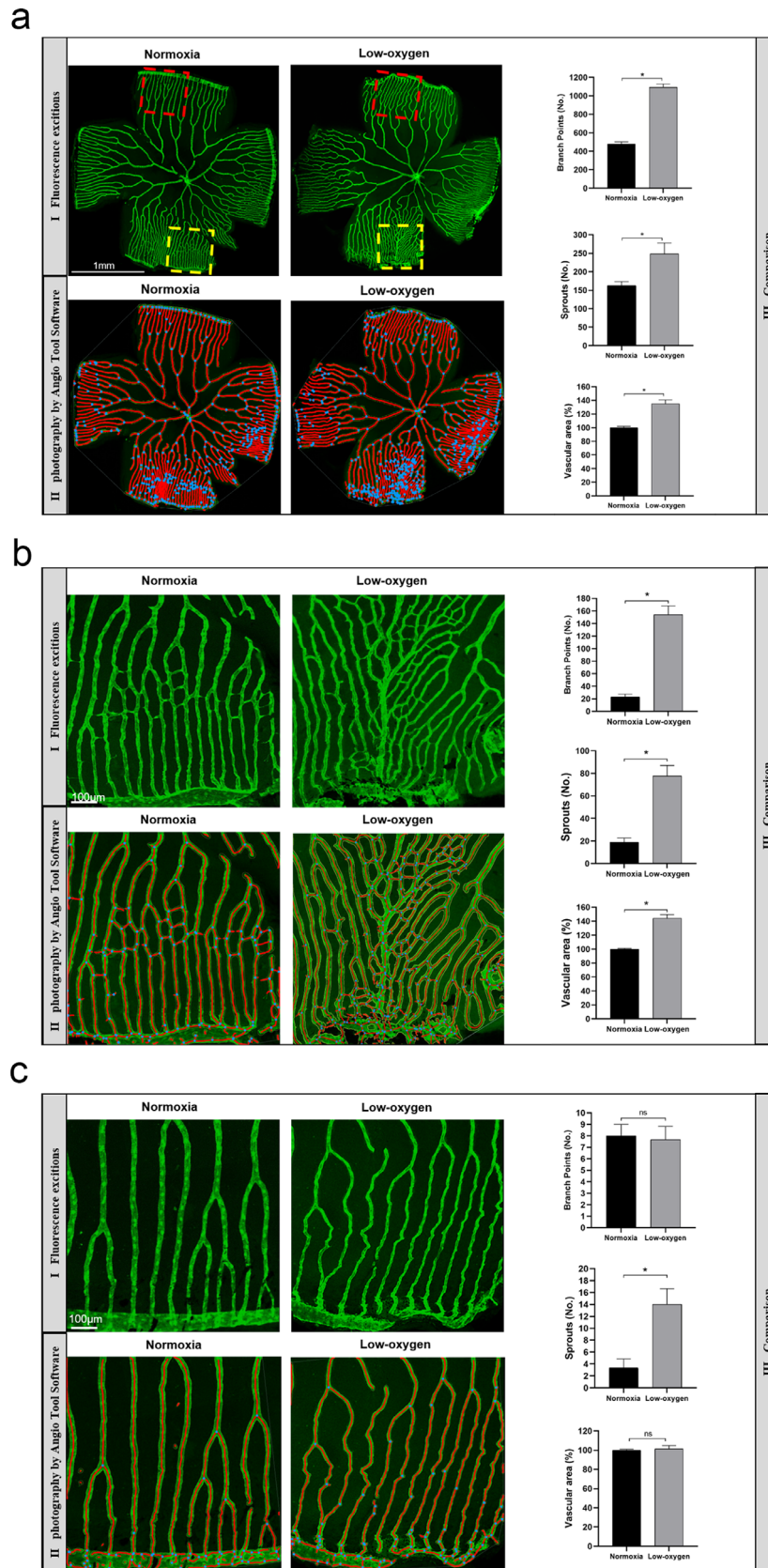


**FIGURE 7. Comparison of low oxygen-induced retinal neovascularization in adult zebrafish.** (A) Confocal microscopic observation of total retinal vessels in adult zebrafish. (B) Confocal microscopic observation of high vascularity areas of the retina (within the 350  $\mu\text{m}$  square yellow area in panels A–I) in adult zebrafish. (C) Confocal microscopic observation of low vascularity areas of the retina (within the 350  $\mu\text{m}$  square red area in panels A–I) in adult zebrafish. (I) Fluorescence excitation; (II) Photography by Angio Tool Software. The outline of the vasculature is shown in yellow, the skeleton representation of vasculature in red and branching points are blue; (III) comparison of vessel branch points, sprouts, and vascular area. \* Significant difference compared with the normoxia group (paired *t*-test, *P* values < 0.05).

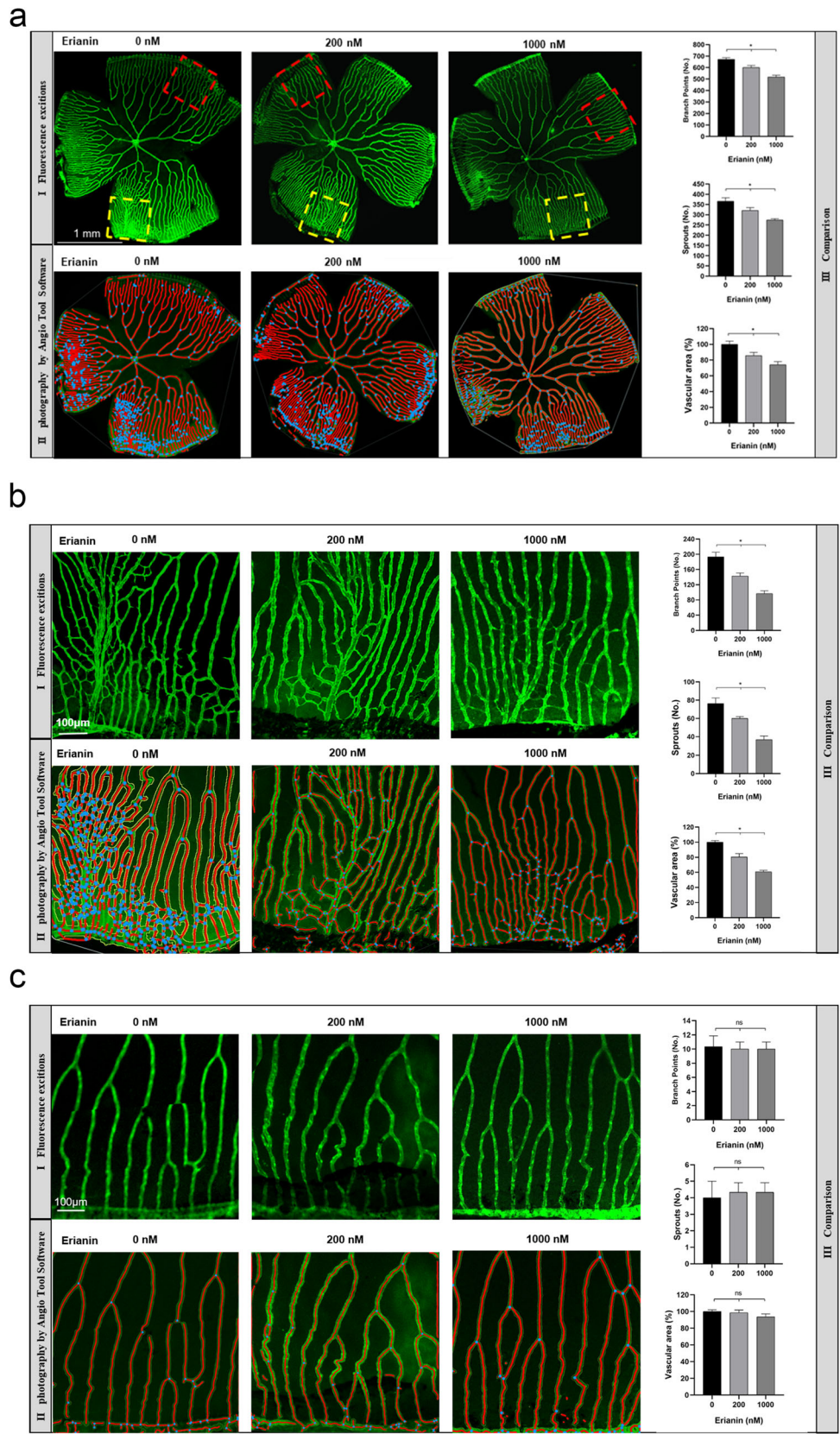


**FIGURE 8. Effect of erianin on low oxygen-induced retinal neovascularization in adult zebrafish.** (A) Confocal microscopic observation of total retinal vessels in adult zebrafish treated with erianin (200 nM and 1000 nM). (B) Confocal microscopic observation of high vascularity areas of the retina (within the 350  $\mu\text{m}$  square yellow area in panels A–D) in adult zebrafish treated with erianin (200 nM and 1000 nM). (C) Confocal microscopic observation of low vascularity areas of the retina (within the 350  $\mu\text{m}$  square red area in panels A–D) in adult zebrafish treated with erianin (200 nM and 1000 nM). (D) Fluorescence excitation; (II) Photography by Angio Tool Software. The outline of the vasculature is shown in yellow, the skeleton representation of vasculature in red and branching points are blue; (III) Comparison of vessel branch points, sprouts, and vascular area. \* Significant difference compared with normoxia group (paired *t*-test, *P* values < 0.05).

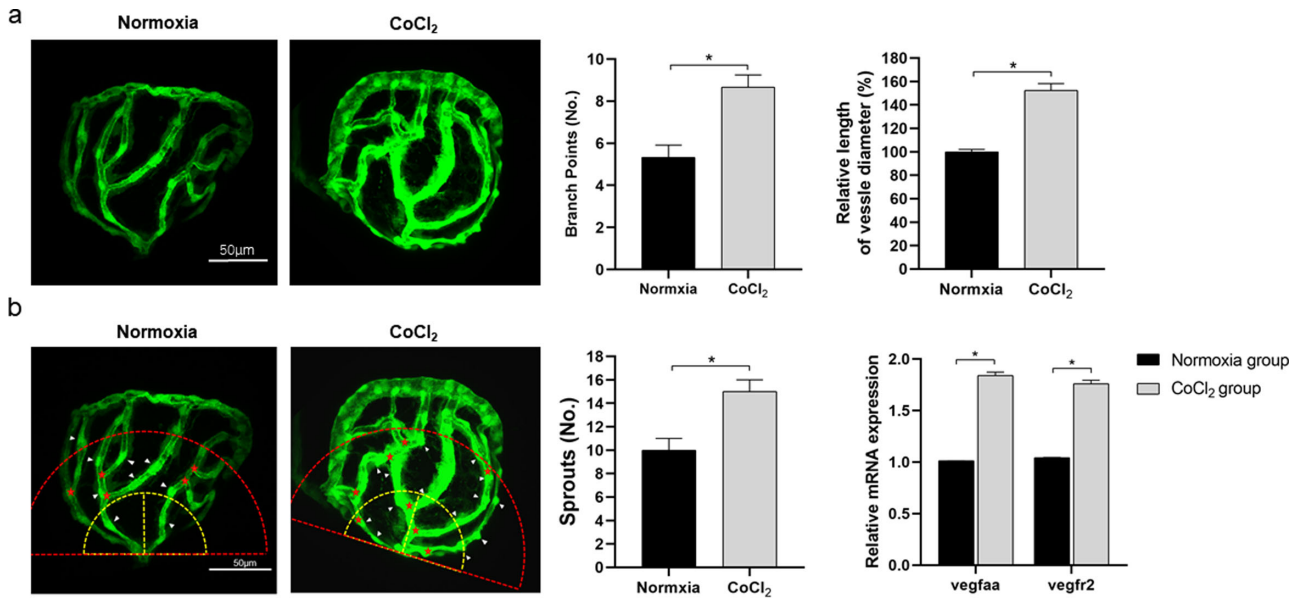


**FIGURE 9. Comparison of CoCl<sub>2</sub>-induced retinal neovascularization in zebrafish embryos.** (A) With fluorescence excitation, excessive retinal vascularization was shown in 5 mM CoCl<sub>2</sub>-treated embryos compared with the untreated control at the same developmental stage. (B) The method of counting branch points (*red asterisks*), vessel sprouts (*white arrowheads*) within a red semicircle with a radius of 100 μm, and measuring the mean diameter of the retinal vessels proximal to the optic disc (within the *yellow semicircle* with a radius of 50 μm). Comparison of branch points, vessel diameter and sprouts. mRNA expression of *vegfaa* and *vegfr2* in the retinas of zebrafish embryos. \* Significant difference compared with the normoxia group (independent sample *t*-test, *P* values < 0.05).

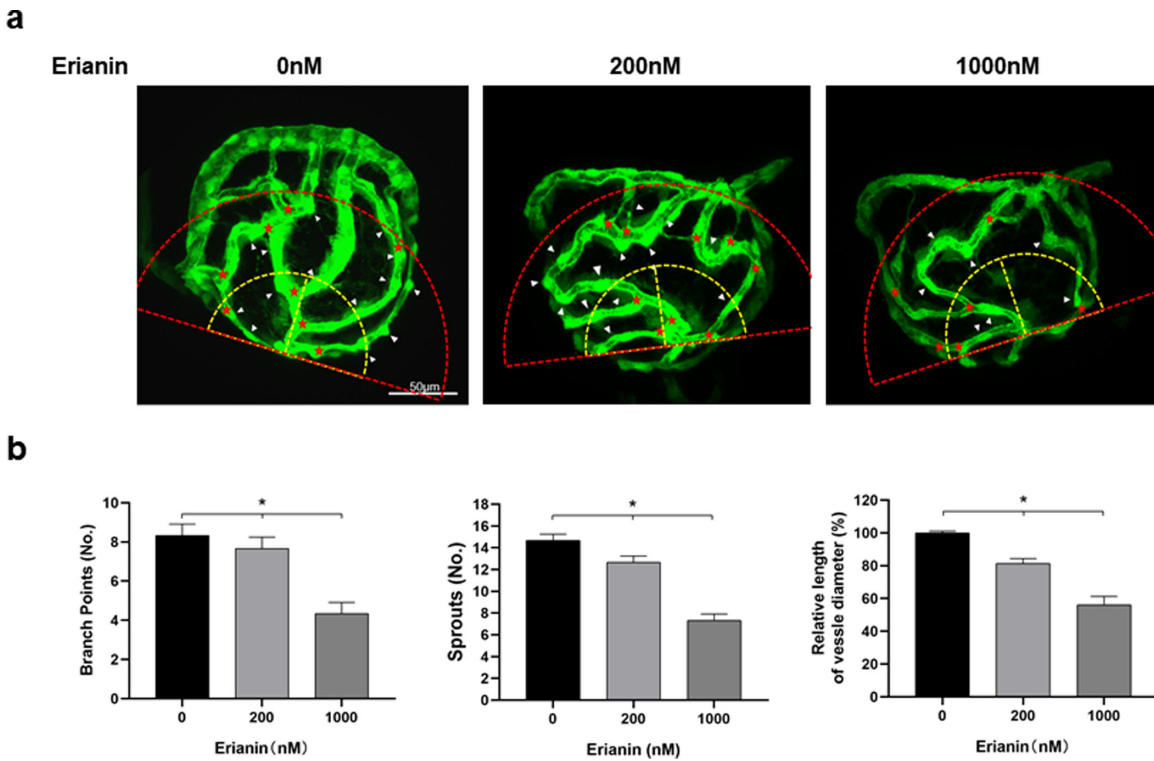


**FIGURE 10. Effect of erianin on CoCl<sub>2</sub>-induced retinal neovascularization in zebrafish embryos.** (A) Confocal microscopic observation of retinal vessels in zebrafish embryos treated with erianin at various concentrations (0, 200, and 1000 nM). The panels show the method for counting vessel branch points (*red asterisks*), sprouts (*white arrowheads*) within the *red semicircle* with a radius of 100 μm, and measuring the mean diameter of the retinal vessels proximal to the optic disc (within the *yellow semicircle* with a radius of 50 μm). (B) Comparison of branch points, vessel diameter, and sprouts. \* Significant difference among samples after multiple comparisons (SNK-q test, *P* values < 0.05).

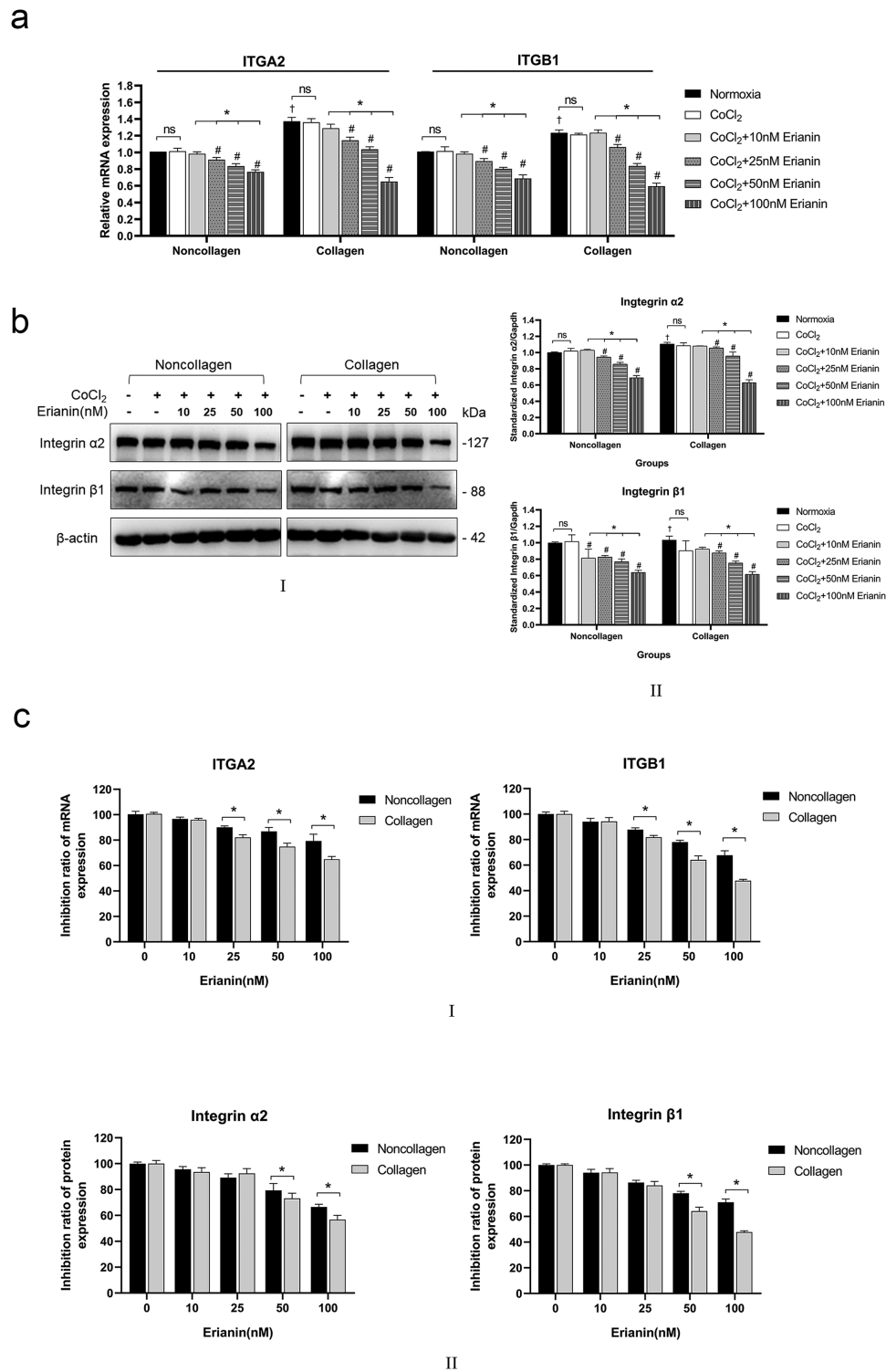


**FIGURE 11. Effects of erianin on  $\alpha 2$  and  $\beta 1$  integrins in vitro.** (A) The mRNA levels of ITGA2 and ITGB1 in HRVECs exposed to normoxia, CoCl<sub>2</sub>, or erianin at various concentrations. (B) (B–I) Protein levels of  $\alpha 2$  and  $\beta 1$  integrins in HRVECs exposed to normoxia, CoCl<sub>2</sub>, or erianin at various concentrations. (B–II) Quantitative analysis of  $\alpha 2$  and  $\beta 1$  integrins; the results are presented as percentages of the normoxia group. (C) (C–I) The inhibition ratios of ITGA2 and ITGB1 were compared between hypoxic HRVECs cultured under collagen and noncollagen conditions and treated with erianin at various concentrations. (C–II) The inhibition ratios of  $\alpha 2$  and  $\beta 1$  integrin proteins were compared between hypoxic HRVECs cultured under collagen and noncollagen conditions and treated with erianin at various concentrations. Hypoxic cells without erianin treatment were set as controls at 100%. \* Significant difference between samples (paired *t*-test, *P* values < 0.05); † Comparison with the noncollagen group of CoCl<sub>2</sub>-incubated cells without erianin treatment (paired *t*-test, *P* values < 0.05); § Significant difference between collagen and noncollagen groups (independent sample *t*-test, *P* values < 0.05; ITGA2: integrin subunit alpha 2 [human]; ITGB1: integrin subunit beta 1 [human]).

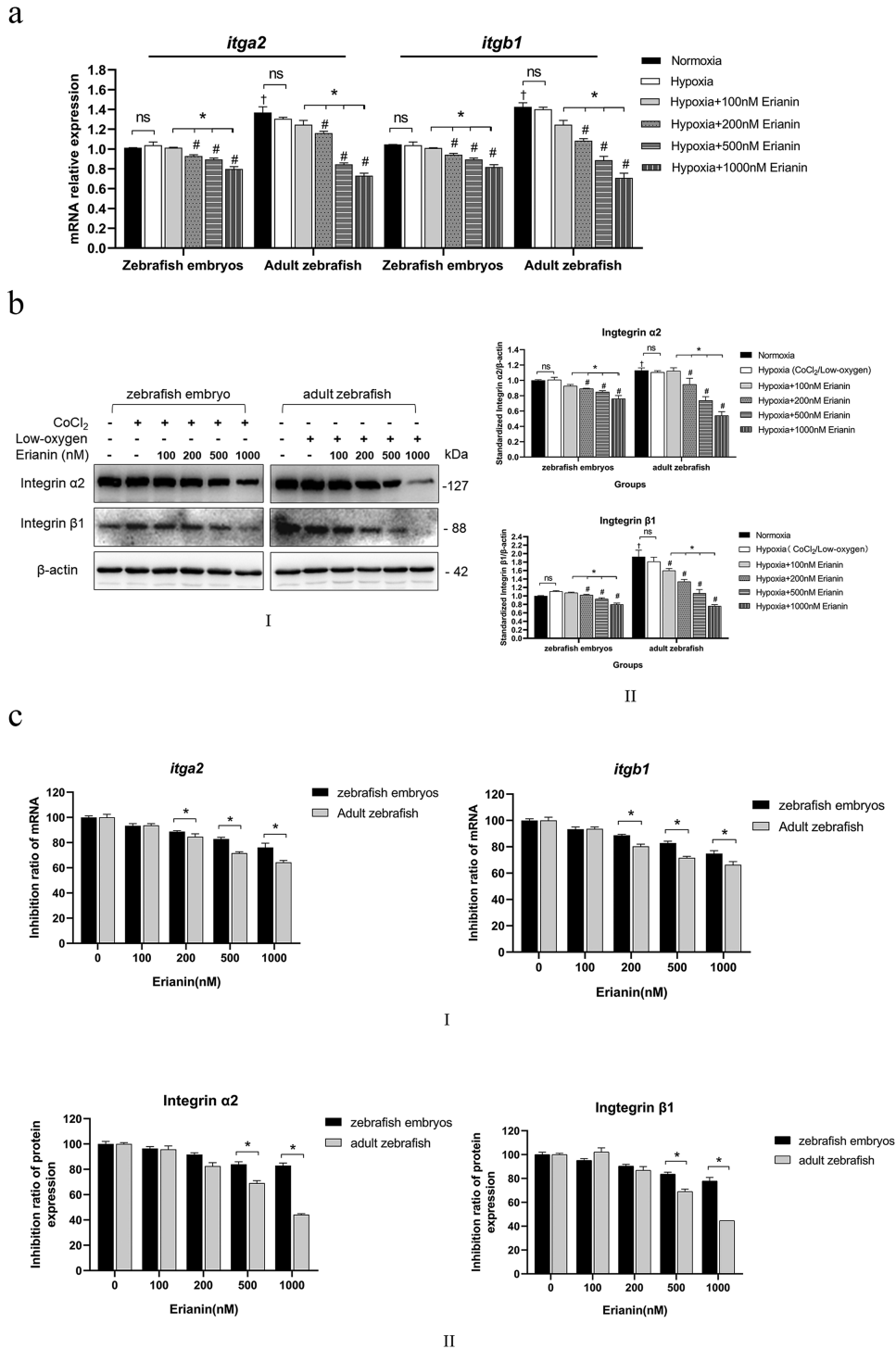
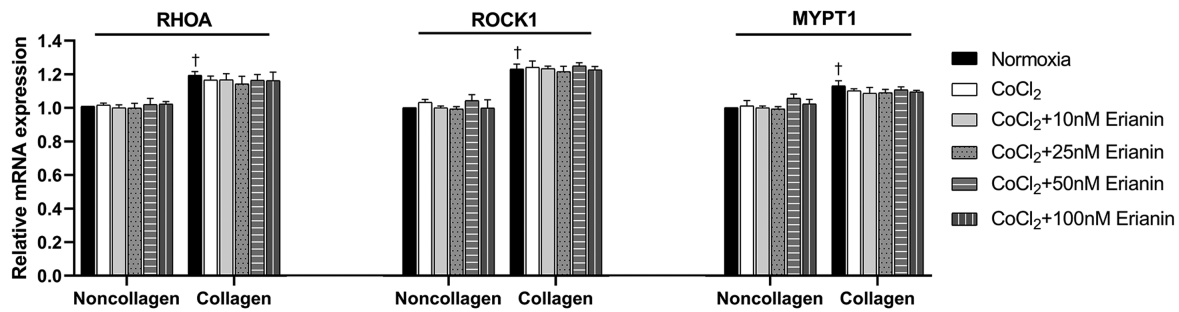


**FIGURE 12. Effects of erianin on  $\alpha 2$  and  $\beta 1$  integrins in vivo.** (A) mRNA levels of *itga2* and *itgb1* in adult and embryonic zebrafish retinas exposed to normoxia, hypoxia, or erianin at various concentrations. (B) (B–I) Protein levels of  $\alpha 2$  and  $\beta 1$  integrins in the retinas of adult and embryonic zebrafish under normoxia, hypoxia, or erianin at various concentrations. (B–II) Quantitative analysis of  $\alpha 2$  and  $\beta 1$  integrins; the results are presented as percentages of the normoxia group. (C) (C–I) The inhibition ratios of *itga2* and *itgb1* were compared between low-oxygen induced adult zebrafish and CoCl<sub>2</sub>-induced zebrafish embryos. (C–II) The inhibition ratios of  $\alpha 2$  and  $\beta 1$  integrin proteins were compared between hypoxia-induced adult zebrafish and CoCl<sub>2</sub>-induced zebrafish embryos and treated with erianin at various concentrations. Low-oxygen induced adult zebrafish and CoCl<sub>2</sub>-induced zebrafish embryos without erianin treatment were set as controls at 100%. \* Significant difference ( $P$  values < 0.05) between samples in the adult zebrafish (paired  $t$ -test) in A, in the zebrafish embryos (independent sample  $t$ -test) in B, and between adult zebrafish and zebrafish embryos (independent sample  $t$ -test) in C; # Comparison with adult zebrafish induced by low oxygen without erianin treatment (paired  $t$ -test,  $P$  values < 0.05) or with zebrafish embryos induced by CoCl<sub>2</sub> without erianin treatment (independent sample  $t$ -test,  $P$  values < 0.05); † Comparison with normoxia zebrafish embryos without erianin treatment (independent sample  $t$ -test,  $P$  values < 0.05); (*itga2*: integrin subunit alpha 2 [zebrafish]; *itgb1*: integrin subunit beta 1 [zebrafish]).

a



b

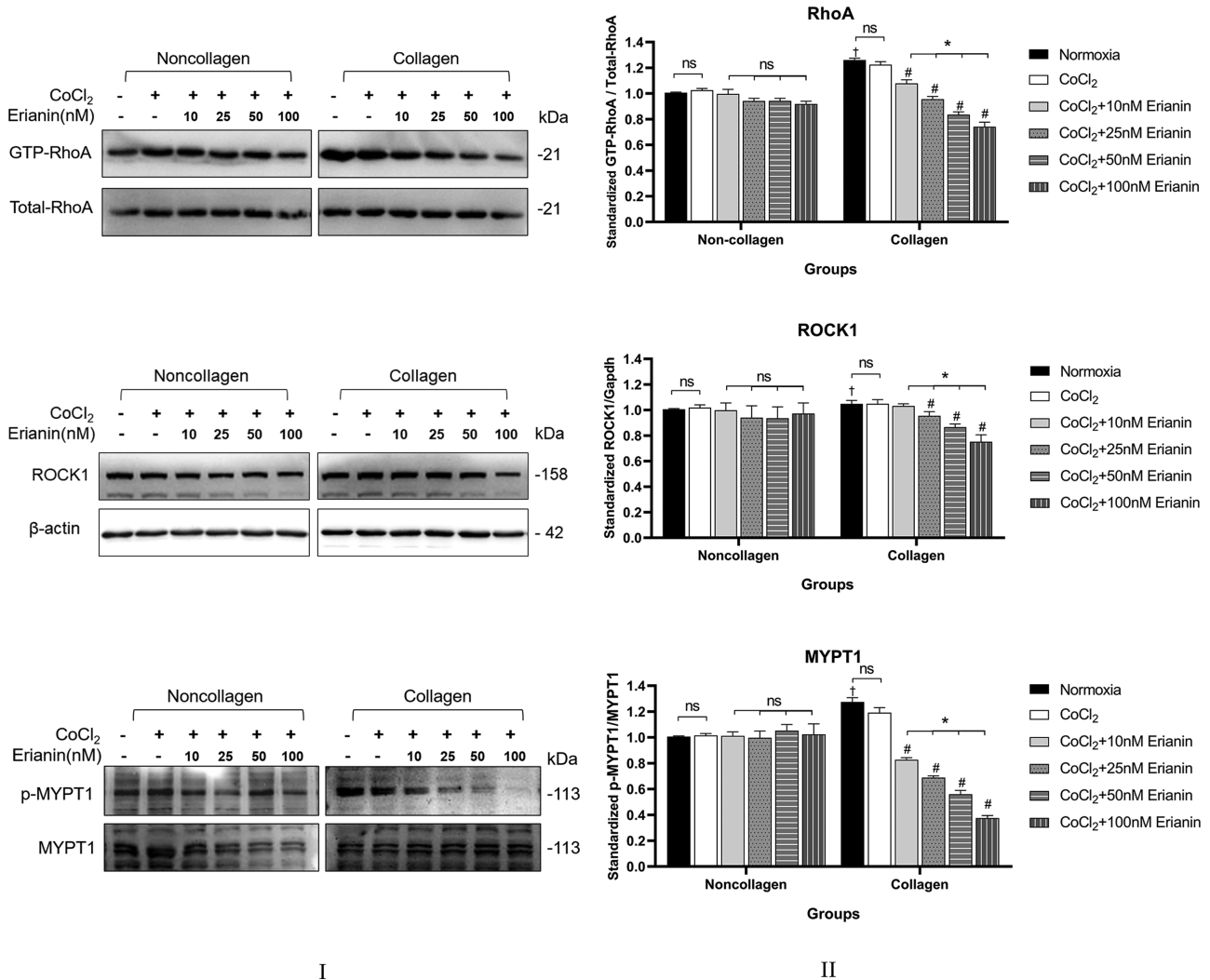


**FIGURE 13. Effects of erianin on the RhoA/ROCK1 pathway in vitro.** (A) The mRNA levels of RHOA, ROCK1, and MYPT1 in HRVECs exposed to normoxia, CoCl<sub>2</sub>, or erianin at various concentrations. (B) (B-I) Protein levels of GTP-RhoA, ROCK1, and p-MYPT1 in HRVECs exposed to normoxia, CoCl<sub>2</sub>, or erianin at various concentrations. (B-II) Quantitative analysis of GTP-RhoA, ROCK1, and p-MYPT1; the results are presented as percentages of the normoxia group. \* Significant difference between samples (paired *t*-test, *P* values < 0.05); # Comparison with the collagen group of CoCl<sub>2</sub>-incubated cells without erianin treatment (paired *t*-test, *P* values < 0.05); † Comparison with noncollagen group of normoxia cells without erianin treatment (independent sample *t*-test, *P* values < 0.05).



## DISCUSSION

Previous studies have shown that erianin has anticancer activity<sup>32-34</sup> and inhibited angiogenesis in vivo and in vitro.<sup>13,14</sup> Erianin also inhibited high glucose-induced retinal angiogenesis by blocking the ERK1/2-regulated HIF-1 $\alpha$ -VEGF/VEGFR2 pathway.<sup>15</sup> Although anti-VEGF therapy has become the standard treatment for retinal neovascularization, many patients do not respond adequately to this therapy. Therefore, developing agents that inhibit retinal neovascularization through different pathways will hopefully provide a promising therapeutic strategy. The vitreous plays an important role in pathological retinal angiogenesis.<sup>35,36</sup> In this research, we used cell models in vitro and zebrafish models in vivo to mimic neovascularization, and observed the effects of erianin on retinal neovascularization in collagen in both in vitro and in vivo.

In the present study, the concentration-dependent effects of erianin on hypoxic cells but had no significant inhibitory effect on normoxic cells, which may be because the cellular target receptor of erianin was not activated in the normoxic environment. In the hypoxic cell model, erianin significantly inhibited cell proliferation, migration, tube formation, and adhesion in a concentration-dependent manner, and the inhibitory effect of cell proliferation and tube formation was more evident in the collagen group. Comparison of the effects of erianin in cell migration and cell adhesion assays could not be performed due to the inconsistent environments of adherent cultures and 3D collagen cultures, which will be further investigated in a subsequent study. This finding suggested that erianin selectively inhibits collagen-mediated neovascularization, likely because erianin only interferes with the interaction between collagen and cells. Consequently, the inhibitory effect of erianin was not fully functional in the environment without collagen. These results demonstrate that erianin plays a crucial inhibitory role in the proangiogenic effects on collagen.

A model of hypoxia-induced retinal neovascularization in zebrafish was used to assess the inhibitory effect of erianin on retinal neovascularization in vivo. Because there was no vitreal space in embryonic zebrafish,<sup>26</sup> they were used as an in vivo neovascularization model for the low collagen environment in this study. Our study successfully established a CoCl<sub>2</sub>-induced retinal neovascularization model in zebrafish embryos by exposing zebrafish embryos to CoCl<sub>2</sub> based on previous studies.<sup>22</sup> In addition, a previous study successfully induced retinal hypoxia by intraocular injection of CoCl<sub>2</sub> into adult zebrafish vitreous.<sup>37</sup> However, because multiple intraocular injections increase the risk of complications and repeated anesthesia can also reduce the survival rate of zebrafish in this method. We therefore chose to construct a hypoxic zebrafish retinal model by reducing the oxygen content in the water based on previous studies.<sup>27</sup> This model has been applied in a variety of fields, such as oncology,<sup>38</sup> cardiovascular,<sup>39</sup> and ophthalmology,<sup>40,41</sup> and has been successfully used to screen for small molecule antiangiogenic compounds.<sup>42</sup> Our study demonstrated that erianin inhibited retinal neovascularization in a concentration-dependent manner in both adult zebrafish and zebrafish embryos models. However, there was no statistical difference in the thickness of the zebrafish retinal vessels. Thus, further studies with expanded samples size should be done to address this issue. To explore the mechanism by which erianin inhibition of collagen promotes neovascularization, this study revealed significant increase in the protein and mRNA levels of  $\alpha 2$  and  $\beta 1$

integrins.  $\alpha 2\beta 1$  integrin was identified as an ECM receptor for collagens.<sup>43</sup> Collagen signals into endothelial cells via integrins and activates cells. Intracellular responses include increased RhoA/ROCK1 signaling activity.<sup>35,44,45</sup> RhoA binds ROCK, which leading to the phosphorylation of MYPT1 and the increase of actomyosin contractility.<sup>46,47</sup> The Rho family of small GTPases play pivotal roles in the control of cytoskeletal rearrangements, cell-matrix adhesions, and cell-cell junctions in endothelial cells, thereby regulating vascular formation and permeability.<sup>44,48,49</sup> The present study shows that erianin inhibits the transcription and translation of collagen-activated  $\alpha 2$  and  $\beta 1$  integrins. However, in vitro assays showed that erianin inhibited collagen-activated RhoA/ROCK1 pathway activity only in the collagen group. In vivo experiments in zebrafish also showed that the inhibitory effect of erianin on RhoA/ROCK1 pathway activity was more evident in adult zebrafish eyes containing more vitreous collagen than in embryonic zebrafish eyes. It suggests that erianin may have an effect on the intracellular transactivation pathway via inhibition of the expression of collagen-bound integrins.

In the present study, the inhibitory effect of erianin on retinal vasculature in vitreous-containing zebrafish was more pronounced than in vitreous-free zebrafish, suggesting that erianin inhibits neovascularization more significantly in the presence of collagen than in the absence of collagen. This suggests that the inhibition of intraocular neovascularization by erianin may be related to the collagen. The mechanism of collagen interference has not been further elaborated in this study, which is subject to further research. In this paper, we analyzed the unique receptor for collagen in the vascular endothelial cell membrane, "integrin," and the downstream signaling pathway after integrin activation. The results showed that erianin significantly inhibited integrins and downstream signaling pathways. Because integrins are the only receptors that bind collagen, the inhibition of neovascularization in the collagen environment by erianin is evident.

In summary, our data provide compelling evidence that erianin is an important regulator of pathological angiogenesis in both in vitro hypoxia-induced cell models and in vivo hypoxia-induced retinal neovascularization models by inhibiting collagen binding to  $\alpha 2$  and  $\beta 1$  integrins and suppressing the intracellular RhoA/ROCK1 signaling pathway. These findings suggest that erianin has therapeutic potential for intraocular collagen-mediated retinal angiogenesis, which remains to be further analyzed in animal disease models and clinical applications.

## Acknowledgments

Supported by grants from the National Natural Science Foundation of Guangdong, China (grant number 2020A1515010190) and the Science and Technology Program of Guangzhou, China (grant number 202102010274) and the Project of Traditional Chinese Medicine of Guangdong Province of China (grant number 20201065).

Disclosure: **X. Li**, None; **X. Liu**, None; **Y. Xing**, None; **L. Zeng**, None; **X. Liu**, None; **H. Shen**, None; **J. Ma**, None

## References

- Sottile J. Regulation of angiogenesis by extracellular matrix. *Biochim Biophys Acta*. 2004;1654(1):13–22.
- Fibronectins Hynes RO. *Sci Am*. 1986;254(6):42–51.

3. George EL, Baldwin HS, Hynes RO. Fibronectins are essential for heart and blood vessel morphogenesis but are dispensable for initial specification of precursor cells. *Blood*. 1997;90(8):3073–3081.
4. George EL, Georges-Labouesse EN, Patel-King RS, Rayburn H, Hynes RO. Defects in mesoderm, neural tube and vascular development in mouse embryos lacking fibronectin. *Development*. 1993;119(4):1079–1091.
5. Maragoudakis ME, Missirlis E, Karakiulakis GD, Sarmonica M, Bastakis M, Tsopanoglou N. Basement membrane biosynthesis as a target for developing inhibitors of angiogenesis with anti-tumor properties. *Kidney Int*. 1993;43(1):147–150.
6. Kim S, Bell K, Mousa SA, Varner JA. Regulation of angiogenesis in vivo by ligation of integrin alpha5beta1 with the central cell-binding domain of fibronectin. *Am J Pathol*. 2000;156(4):1345–1362.
7. Bishop PN, Holmes DF, Kadler KE, McLeod D, Bos KJ. Age-related changes on the surface of vitreous collagen fibrils. *Invest Ophthalmol Vis Sci*. 2004;45(4):1041–1046.
8. Bishop PN. Structural macromolecules and supramolecular organisation of the vitreous gel. *Prog Retin Eye Res*. 2000;19(3):323–344.
9. Senger DR, Angiogenesis Davis GE. *Cold Spring Harb Perspect Biol*. 2011;3(8):a005090.
10. Xing Y, Li X-K, Lu S-D, Ma J. Regulation of opticin on bioactivity of retinal vascular endothelial cells cultured in collagen. *Int J Ophthalmol*. 2020;13(8):1202–1209.
11. Madamanchi A, Santoro SA, Zutter MM. alpha2/beta1 Integrin. *Adv Exp Med Biol*. 2014;819:41–60.
12. Pharmacopoeia of the People's Republic of China (authors). Pharmacopoeia of the People's Republic of China volumes 1 & 2 (English Edition). Washington, DC: Chemical Industry Press; 2021.
13. Su C, Zhang P, Liu J, Cao Y. Erianin inhibits indoleamine 2, 3-dioxygenase -induced tumor angiogenesis. *Biomed Pharmacother*. 2017;88:521–528.
14. Gong Y-Q, Fan Y, Wu D-Z, Yang H, Hu Z-B, Wang Z-T. In vivo and in vitro evaluation of erianin, a novel anti-angiogenic agent. *Eur J Cancer*. 2004;40(10):1554–1565.
15. Yu Z, Zhang T, Gong C, et al. Erianin inhibits high glucose-induced retinal angiogenesis via blocking ERK1/2-regulated HIF-1alpha-VEGF/VEGFR2 signaling pathway. *Sci Rep*. 2016;6:34306.
16. Chen JX, Zhao T, Huang DX. Protective effects of edaravone against cobalt chloride-induced apoptosis in PC12 cells. *Neurosci Bull*. 2009;25(2):67–74.
17. Lan AP, Ziao L-C, Yang Z-L, et al. Interaction between ROS and p38MAPK contributes to chemical hypoxia-induced injuries in PC12 cells. *Mol Med Rep*. 2012;5(1):250–255.
18. Sandner P, Wolf K, Bergmaier U, Gess B, Kurtz A. Hypoxia and cobalt stimulate vascular endothelial growth factor receptor gene expression in rats. *Pflugers Arch*. 1997;433(6):803–808.
19. Tan CB, Gao M, Xu WR, Yang XY, Zhu XM, Du GH. Protective effects of salidroside on endothelial cell apoptosis induced by cobalt chloride. *Biol Pharm Bull*. 2009;32(8):1359–1363.
20. Zou W, Yan M, Xu W, et al. Cobalt chloride induces PC12 cells apoptosis through reactive oxygen species and accompanied by AP-1 activation. *J Neurosci Res*. 2001;64(6):646–653.
21. Han S, Zhang D, Dong Q, Wang X, Wang L. Deficiency in Neuroserpin Exacerbates CoCl2 Induced Hypoxic Injury in the Zebrafish Model by Increased Oxidative Stress. *Front Pharmacol*. 2021;12:632662.
22. Wu Y-C, Chang C-Y, Kao A, et al. Hypoxia-induced retinal neovascularization in zebrafish embryos: a potential model of retinopathy of prematurity. *PLoS One*. 2015;10(5):e0126750.
23. Chandel NS, Maltepe E, Goldwasser E, Mathieu CE, Simon MC, Schumacker PT. Mitochondrial reactive oxygen species trigger hypoxia-induced transcription. *Proc Natl Acad Sci USA*. 1998;95(20):11715–11720.
24. Befani C, Mylonis I, Gkotiakou I-M, et al. Cobalt stimulates HIF-1-dependent but inhibits HIF-2-dependent gene expression in liver cancer cells. *Int J Biochem Cell Biol*. 2013;45(11):2359–2368.
25. Kajimura S, Aida K, Duan C. Understanding hypoxia-induced gene expression in early development: in vitro and in vivo analysis of hypoxia-inducible factor 1-regulated zebra fish insulin-like growth factor binding protein 1 gene expression. *Mol Cell Biol*. 2006;26(3):1142–1155.
26. Maritan SM, Lian EY, Mulligan LM. An Efficient and Flexible Cell Aggregation Method for 3D Spheroid Production. *J Vis Exp*. 2017;(121):55544.
27. Cao Z, Jensen LD, Rouhi P, et al. Hypoxia-induced retinopathy model in adult zebrafish. *Nat Protoc*. 2010;5(12):1903–1910.
28. Svoboda P, Stein P, Hayashi H, Schultz RM. Selective reduction of dormant maternal mRNAs in mouse oocytes by RNA interference. *Development*. 2000;127(19):4147–4156.
29. Mikelis CM, Palmby TR, Simaan M, et al. PDZ-RhoGEF and LARG are essential for embryonic development and provide a link between thrombin and LPA receptors and Rho activation. *J Biol Chem*. 2013;288(17):12232–12243.
30. Mikelis CM, Simaan M, Ando K, et al. RhoA and ROCK mediate histamine-induced vascular leakage and anaphylactic shock. *Nat Commun*. 2015;6:6725.
31. Munoz-Sanchez J, Chanez-Cardenas ME. The use of cobalt chloride as a chemical hypoxia model. *J Appl Toxicol*. 2019;39(4):556–570.
32. Zhang Y, Zhang Q, Wei F, Liu N. Progressive study of effects of erianin on anticancer activity. *Onco Targets Ther*. 2019;12:5457–5465.
33. Yang L, Hu Y, Zhou G, Chen Q, Song Z. Erianin suppresses hepatocellular carcinoma cells through down-regulation of PI3K/AKT, p38 and ERK MAPK signaling pathways. *Biosci Rep*. 2020;40(7):BSR20193137.
34. Liu Y-T, Hsieh M-J, Lin J-T, et al. Erianin induces cell apoptosis through ERK pathway in human nasopharyngeal carcinoma. *Biomed Pharmacother*. 2019;111:262–269.
35. Bishop PN. The role of extracellular matrix in retinal vascular development and preretinal neovascularization. *Exp Eye Res*. 2015;133:30–36.
36. Nawaz IM, Rezzola S, Cancarini A, et al. Human vitreous in proliferative diabetic retinopathy: Characterization and translational implications. *Prog Retin Eye Res*. 2019;72:100756.
37. Medrano MP, Fuster AP, Sanchis PA, Paez N, Bernabeu RO, Faillace MP. Characterization of proliferative, glial and angiogenic responses after a CoCl2 -induced injury of photoreceptor cells in the adult zebrafish retina. *Eur J Neurosci*. 2018;48(9):3019–3042.
38. Lee SLC, Rouhi P, Jensen LD, et al. Hypoxia-induced pathological angiogenesis mediates tumor cell dissemination, invasion, and metastasis in a zebrafish tumor model. *Proc Natl Acad Sci USA*. 2009;106(46):19485–19490.
39. Parente V, Balasso S, Pompilio G, et al. Hypoxia/reoxygenation cardiac injury and regeneration in zebrafish adult heart. *PLoS One*. 2013;8(1):e53748.
40. Ali Z, Mukwaya A, Biesemeier A, et al. Intussusceptive Vascular Remodeling Precedes Pathological Neovascularization. *Arterioscler Thromb Vasc Biol*. 2019;39(7):1402–1418.
41. Jensen LD, Rouhi P, Cao Z, Länne T, Wahlberg E, Cao Y. Zebrafish models to study hypoxia-induced pathological

- angiogenesis in malignant and nonmalignant diseases. *Birth Defects Res C Embryo Today*. 2011;93(2):182–193.
42. Cao R, Jensen LD, Söll I, Hauptmann G, Cao Y. Hypoxia-induced retinal angiogenesis in zebrafish as a model to study retinopathy. *PLoS One*. 2008;3(7):e2748.
  43. Emsley J, Knight CG, Farndale RW, Barnes MJ, Liddington RC. Structural basis of collagen recognition by integrin alpha2/beta1. *Cell*. 2000;101(1):47–56.
  44. Uemura A, Fukushima Y. Rho GTPases in Retinal Vascular Diseases. *Int J Mol Sci*. 2021;22(7):3684.
  45. Zahra FT, Sajib MS, Ichiyama Y, et al. Endothelial RhoA GTPase is essential for in vitro endothelial functions but dispensable for physiological in vivo angiogenesis. *Sci Rep*. 2019;9(1):11666.
  46. Jaffe AB, Hall A. Rho GTPases: biochemistry and biology. *Annu Rev Cell Dev Biol*. 2005;21:247–269.
  47. Riento K, Ridley AJ. Rocks: multifunctional kinases in cell behaviour. *Nat Rev Mol Cell Biol*. 2003;4(6):446–456.
  48. Bryan BA, D'Amore PA. What tangled webs they weave: Rho-GTPase control of angiogenesis. *Cell Mol Life Sci*. 2007;64(16):2053–2065.
  49. van der Meel R, Symons MH, Kudernatsch R, et al. The VEGF/Rho GTPase signalling pathway: a promising target for anti-angiogenic/anti-invasion therapy. *Drug Discov Today*. 2011;16(5-6):219–228.